

Band structure and optical parameters of the SnO₂(110) surface

Matti A. Mäki-Jaskari and Tapio T. Rantala

Institute of Physics, Tampere University of Technology, P.O. Box 692, FIN-33101 Tampere, Finland

(Received 29 January 2001; published 23 July 2001)

With a first-principles-density-functional method, combined with two different pseudopotentials, ideal oxidized and reduced surfaces of tin oxide are studied. The band structures of bulk and the surface systems are calculated and compared. The nature of the surface Sn²⁺ ions, their outward relaxation, associated “dangling bonds” and band gap states are considered. Also ultraviolet optical constants are determined by using the electric dipole approximation with a scissor correction, and noted to agree with experiments. The presence of the surface, and more significantly, its removed bridging oxygen atoms, becomes apparent in a formation of a new absorption feature. This is predicted to cause about 0.7 eV decrease of the absorption edge.

DOI: 10.1103/PhysRevB.64.075407

PACS number(s): 73.20.-r, 68.35.-p, 78.20.-e, 78.68.+m

I. INTRODUCTION

Polycrystalline tin oxide (SnO₂, cassiterite) and thin films of unique properties and of high quality can be prepared by techniques such as chemical vapor deposition, spray pyrolysis, evaporation, and sputtering.^{1,2} This material has found a wide range of applications in electric equipments and coatings where transparency is required, and more recently, also in gas sensors. In the present state of research, difficulties are met in the accurate experimental determination of the structure of its surfaces due to both dependence of preparation conditions of the samples and due to need of nonconventional measurement techniques.^{3,4} Therefore, theoretical methods are well suited to gain insight to the surface structure and properties in this connection.⁵⁻¹¹

We will study here the (110) surface of SnO₂, which is the most stable of naturally grown faces of the SnO₂ crystal. For instance, by using crystals obtained by vapor-phase reaction method combined with heating and oxidation treatments, almost perfect oxidized (stoichiometric) SnO₂(110) surface can be prepared.¹² One may also introduce oxygen deficiency to this surface by heating it in vacuum to form the reduced surface.¹² By using theoretical and first principles methods we examine the properties of these two surface structures [shown in Fig. 1(b)] in addition to underlying bulk crystal. The two surface structures are viewed to be unsophisticated prevailing limiting cases. Depending on preparation, tin oxide may also contain defective microstructures and surfaces associated with oxygen deficiency.^{3,13,14}

Qualitatively in the limit of purely ionic approximation, the crystal of SnO₂ is composed of Sn⁴⁺ and O²⁻ ions. Along this approximation, analogously to SnO crystals,¹⁵ at the surfaces of SnO₂ also tin Sn²⁺ ions may be defined to be present. We may thus expect that in SnO₂, Sn²⁺ ions interact less with oxygen atoms due to decreased ionic nature. The valence electrons of Sn²⁺ may also contribute to occupied “dangling bonds,” which we find with charge density and band structure calculations. Interactions in SnO₂ are known to have also significant covalent nature,^{5,16} and thus, the theory of charge sharing and transfer can be further developed.¹⁷ But we conclude here that self-consistent electronic structure calculation is needed to accurately describe the charge distribution at the surfaces.

Our calculations also offer a possibility to interpret optical properties of tin oxide material. While the reflectance of tin oxide near its infrared transparency edge is largely explained by optical phonons,^{1,4} the ultraviolet absorption of this wide band gap material is more significantly connected to electronic excitations to the conduction band. These properties can be influenced by creation of oxygen vacancies and impurity doping.¹ We utilize the electric dipole approximation¹⁸ to describe ultraviolet optical properties. This approximation is noted to serve well in obtaining a connection between optical properties and structure of tin oxide. In transparent polycrystalline material like tin oxide the surface contribution to the properties can be expected to be enhanced. Therefore, we separately evaluate the bulk and surface optical parameters of SnO₂. This kind of information has recently been found to be important also in attempts to monitor film growth.¹⁹

A description of the computational method is first presented, followed by the models of bulk and surface systems. Next, the discussion is extended to optical properties and in the last section main results of our calculations are briefly summarized.

II. METHOD

The crystal structure and unit cell of SnO₂, consisting of two tin and four oxygen atoms, is shown in Fig. 1(a). In Fig.

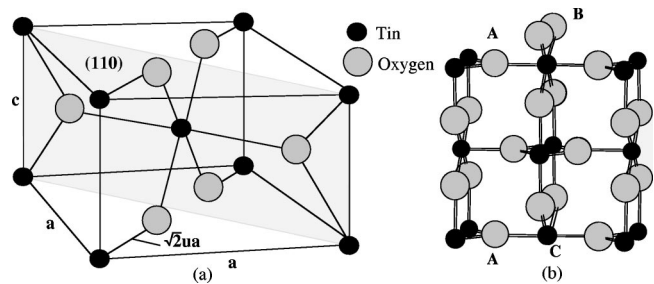


FIG. 1. (a) Primitive unit cell of the bulk cassiterite structure. The shaded plane corresponds to (110) surface. (b) Supercell of the slab model. The top face illustrates the stoichiometric and bottom face the reduced (110) surface. The atom labeled A corresponds to in-plane oxygen, B corresponds to bridging oxygen, and C to the fourfold coordinated tin (Sn²⁺) atom.

1(b) the supercell of corresponding (110) surface slab systems is illustrated. Top face of the supercell illustrates surface terminated by bridging oxygens (stoichiometric surface) and bottom face illustrates surface without oxygen atoms forming the reduced surface. The stoichiometric supercell consists of 18 atoms and the reduced one of 16 atoms. The increase of accuracy by using larger number of atoms, was noted to be relatively small, and the small size of the supercell allowed comparisons to be made with more sophisticated pseudopotential.

Our computational first-principles-density-functional approach is based on the plane wave basis set and pseudopotential concept to describe electron-ion interaction (CASTEP/CETEP code).²⁰ The use of the plane waves is preferred since the results are not strongly tied to the choice of basis set and number of interacting neighbor atoms. Also the periodic boundary conditions are fully taken into account. By using ultrasoft pseudopotentials (USP's) (Refs. 21,22) plane wave basis set can be considerably limited. To check the validity of USP results, many of our results were completely reproduced by using more accurate nonoptimized norm-conserving pseudopotentials (PSP's), which were generated by using the Teter scheme.²³ Oxygen atoms are described by six electrons plus the pseudopotential ion core. Tin atoms contain four electrons in the case of the USP, and 22 electrons in the case of the PSP potential. The electronic interactions were taken into account with generalized-gradient approximation (GGA) as parametrized by Perdew and Wang.²⁴ The self-consistent ground state total energy of the system for all ion positions is obtained by density mixing²⁵ in the case of USP, and by band-by-band technique²⁰ in the case of PSP. The material is treated as insulator and partial occupations of energy levels are not used. Plane waves with kinetic (cutoff) energy higher than 500 eV were not included in the case of USP. However, to check successful convergence in USP bulk geometry optimization, cutoff energies up to 750 eV were used. The PSP requires considerably higher cutoff energy, but we could perform relaxation simulations using cutoff values of 1000 eV and then increase accuracy by to cutoff at 2500 eV.

Integration over the Brillouin zone involved a symmetrized Monkhorst-Pack points.²⁶ For the geometry optimization of unit cell, a set of 6–9 k points seemed to be sufficient and 4–5 for slab relaxation due to the larger unit cell. For geometry optimization, the number of k -point values was also increased to check convergence. Some additional k points with weight zero were included to assist interpolation in the following band structure calculations. In a case of slab model, the vacuum between the surfaces was initially 6 Å, but it needed to be increased to 10 Å in the case of PSP to avoid interaction between surfaces. The underlying bulk system was taken into account by fixing atoms of the (110) atomic plane in the middle of the slab supercell to the positions corresponding the bulk relaxed structure. For all systems the ionic relaxations were carried out with Broyden-Fletcher-Goldfarb-Shanno algorithm.²⁷ As expressed in Table I, calculated bulk lattice parameters coincide closely with experimentally determined lattice parameters,²⁸ which

TABLE I. Calculated bulk lattice parameters (a and c in Å) of cassiterite as defined in Fig. 1. PSP and USP refer to the chosen pseudopotentials.

	a	c	u
Experimental (Ref. 28)	4.74	3.19	0.306
PSP	4.75	3.22	0.306
USP	4.70	3.14	0.306

was one of the main reasons for the pseudopotential choices made.

For each of the structures optical dielectric function calculations with light along [110] were performed. The optical transition matrix elements R are of the form

$$R = \mathbf{Z} \langle f | \mathbf{r} | i \rangle, \quad (1)$$

between the occupied i and unoccupied f states. In Eq. (1) \mathbf{r} is the position operator and vector \mathbf{Z} is the unit vector in the direction of the electric field, perpendicular to the normal of incident light. The electric field was considered to be unpolarized, in which case \mathbf{Z} is taken as an average in the plane of the incident normal. Effects attributed to plasmon excitations, as observed in the maximum of electron energy loss function [$\text{Im}(1/\epsilon)$] of electron energy loss spectroscopy measurements, are not expected to be correctly described by the dipole approximation used.^{4,29,30} However, other optical properties such as absorption and dielectric function are expected to be accounted for. These may be compared to those determined from photoelectron yield spectroscopy³¹ and electron energy loss measurements,³⁰ in addition to direct reflectance and absorption measurements.³²

Calculations of matrix elements R were carried out in the reciprocal space, for which a correction term due to the non-locality of the pseudopotential³³ is included. The number of special k points were doubled compared to energy minimization calculations. The influence of the increase of the number of k points, together with the Gaussian broadening of width 0.6 eV for USP and 0.45 eV for PSP used seems to be quite insignificant. Absorption coefficient $\alpha = 1.02 \times 10^3$ kE (in units 1/cm), which is calculated as in Ref. 30, is obtained from transition energy E (in eV) and optical extinction coefficient k that is calculated from the dielectric function.²⁹ The real part of the dielectric function is obtained from the Kramers-Kronig relation.

We also performed the Mulliken population analysis for the structures, which were calculated by using USP. In this analysis Mulliken charges of atoms and bond populations of pairs are calculated in terms of density matrix and overlap matrix.³⁴ These are obtained from projections of the one-electron eigenfunctions to the atomic orbitals.

III. ELECTRONIC STRUCTURE OF BULK CASSITERITE

We shall here consider briefly the electronic structure of bulk rutile structure crystal of SnO_2 based on our calculations. Contrary to the ionic approximation, valence tin p , s and also d occupancies can be significant.^{6,35} We noticed by performing the Mulliken population analysis, that the Sn ions

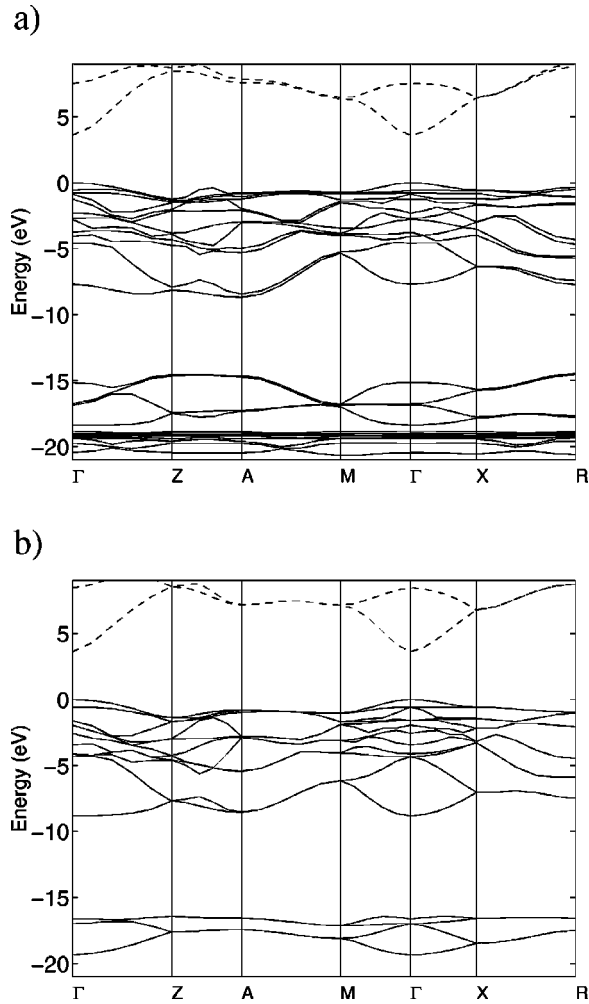


FIG. 2. Band structure of bulk SnO_2 calculated by using PSP (a) and USP (b) pseudopotentials. The path is along the symmetry lines in reciprocal space and allows a direct comparison to earlier calculations (Ref. 8).

have 1.2 s electrons and 1.1 p -electron content. Compared to the earlier calculations³⁵ including d electrons, it seems that the small Sn-valence d -electron content is replaced by s electrons if USP is used. In this respect, the quality of the approximation that ignores this small d content, may be well accepted in systems having symmetric atomic environment. Oxygen atoms were respectively composed of 1.9 s electrons and 5.0 p electrons.

Comparing the width of the upper valence band of the calculated band structure, which is illustrated in Fig. 2, to the experimental result of 7.5 eV,³¹ a slight overestimation is noticed. The width of the PSP valence band is 7.9 eV, while in the case of USP the width is slightly larger, 8.8 eV. The obvious reason for the difference between pseudopotential results is the fact that the accuracy of low valence bands is improved considerably by the explicit treatment of core states of PSP pseudopotential. In both cases we find direct band gap in agreement with experiments. The application of the local density type of approximation is known to underestimate excited state energies. This situation is corrected by using so called scissor operation that simply shifts rigidly the

unoccupied energy levels (by 2.25 eV in the case of USP and 1.92 eV in the case of PSP) to reinstate experimentally known direct bulk band gap (E_g) of SnO_2 . We chose the band gap to be $E_g = 3.6$ eV,² although larger value has been observed in some cases.³⁶ The same shift to the unoccupied levels is applied in all of our calculations discussed below.

The partial densities of states in terms of s - and p -angular momentum projectors for USP is in agreement with earlier interpretations.³⁷ As it is quite typical for metal oxides,⁴ oxygen 2s contributes strongly to the band below -15 eV and O-2p strongly to the whole upper valence band. The part of the valence band, with energy below -5 eV, contains also little Sn-5s type contribution. The valence band with energy above -5 eV, respectively, is contributed by Sn-5p. In the conduction band minimum the dispersion is relatively high and a first density maximum, of mainly Sn- s type, appears at about 8 eV. At higher energies the Sn- p type density is more significant. The band structure of USP agrees satisfactorily with both experimental and more accurate results of PSP, and we continued to more detailed studies by using mainly this pseudopotential, which is computationally much less demanding.

IV. (110) SURFACES

The (110) surface of SnO_2 is composed of different types of atoms. At the stoichiometric surface there are fivefold, and sixfold coordinated bulklike tin atoms, while at the reduced surface the sixfold coordinated tin atoms are turned to fourfold coordinated. Qualitatively, both inward and also outward relaxations of surface ions may be expected to be associated. The occupancy of surface oxygen ions is expected to remain almost unchanged. In the case of reduced surface, that includes Sn^{2+} ions, the occupied tin contribution can be increased, since unoccupied oxygen states have relatively high energy. We suggest that the the Sn^{2+} contribution presents dangling bond characteristics. In order to study the surfaces in more detail, we applied the slab model and determined the 2D surface band structure after relaxation.

We shall first make a quantitative consideration of calculated surface relaxations. Based on these calculations, it is known that at the SnO_2 surface, there are some displacements of atoms from the bulk positions.^{4,6,8,10} Table II illustrates that there is a small variance of these calculated displacements. The relaxations of USP and PSP are very similar, the former slightly underestimating the degree of relaxations. In Table II, we also present the results of Rantala *et al.*⁶ using linear-combination of atomic orbitals method (LCAO) and of Goniakowski *et al.*⁷ using optimized norm-conserving pseudopotential of Lin *et al.*³⁸ (LP). Results of minimal basis set non self-consistent tight-binding method⁸ (TB) are also shown, indicating less good applicability of this method to model surface relaxations, if compared to the density functional methods.

The oxygen atoms, with respect to tin atoms in the same atomic plane, relax outwards. In the case of the reduced surface this displacement is about 0.3–0.4 Å. Likewise, the tin ions marked by C in Fig. 1(b), relax outwards. In a case of stoichiometric surface the outward relaxations range from

TABLE II. Distances and outward relaxations of atoms along [110], from the plane formed by fivefold coordinated surface tin atoms [see Fig. 1(b)] (Ref. 6). Δ_A corresponds to displacement of threefold coordinated in-plane oxygen and Δ_C to displacement of fourfold/sixfold tin, respectively. d_B is the distance of the bridging oxygen from the plane.

Stoichiometric	Δ_A	d_B	Δ_C
PSP	0.26	1.42	0.22
USP	0.25	1.39	0.21
LP (Ref. 7)	0.22	1.46	0.30
LCAO (Ref. 6)	0.25	1.41	0.20
TB (Ref. 8)	0.29	1.37	0.10
Reduced			
PSP	0.33		0.38
USP	0.30		0.22
LP (Ref. 7)	0.26		0.41
LCAO (Ref. 6)	0.40		0.14
TB (Ref. 8)	0.28		-0.05

0.2 to 0.3 Å. Our earlier calculations, made by using the similar PSP pseudopotential approach⁶ are recalculated here with a different slab model. Due to this and other differences such as cutoff energy and number of k points, the relaxations of PSP as introduced here differ slightly. By performing a few computational experiments with differently strained fixed atomic plane, it became evident that the outward displacements of atoms are also considerably dependent on the strain of the surface layers. These phenomena are also expected to have some significance in the chemical properties of tin oxide surfaces.

The PSP, core states are shifted differently in case of the two surfaces, which have a direct influence on surface energetics. The surface energy of the stoichiometric surfaces³⁹ was calculated to be 1.3 J/m² for USP and 1.1 J/m² for PSP. The half of total energy difference between the stoichiometric and reduced slabs that was reduced by the total energy of a free oxygen molecule, was calculated to be 3.5 eV in the case of USP and 2.7 eV in the case of PSP. This can be used to compare surface stability and to estimate the surface reduction energy.^{11,40}

The whole band structure of the slab model, compared to the corresponding projected bulk band structure, is illustrated in Fig. 3(a) for the stoichiometric surface and in Fig. 3(b) for the reduced surface. The alignment of the projected bulk band structure relative to the surface slab band structure is fixed so that the positions of the valence band minimum at Γ point match. The reasoning for this fixing condition is obtained from a band structure calculation that was performed for a thicker reduced slab system consisting more bulklike atoms. With an accuracy better than 0.5 eV, the related bulk projection area would have been obtained by using the thicker slab system. This is also consistent with investigations suggesting that band bending is minimal in this case.^{9,12,31} In the case of the stoichiometric surface the p -type electrons of bridging oxygen atoms contribute most significantly new occupied states at the top of the valence band,

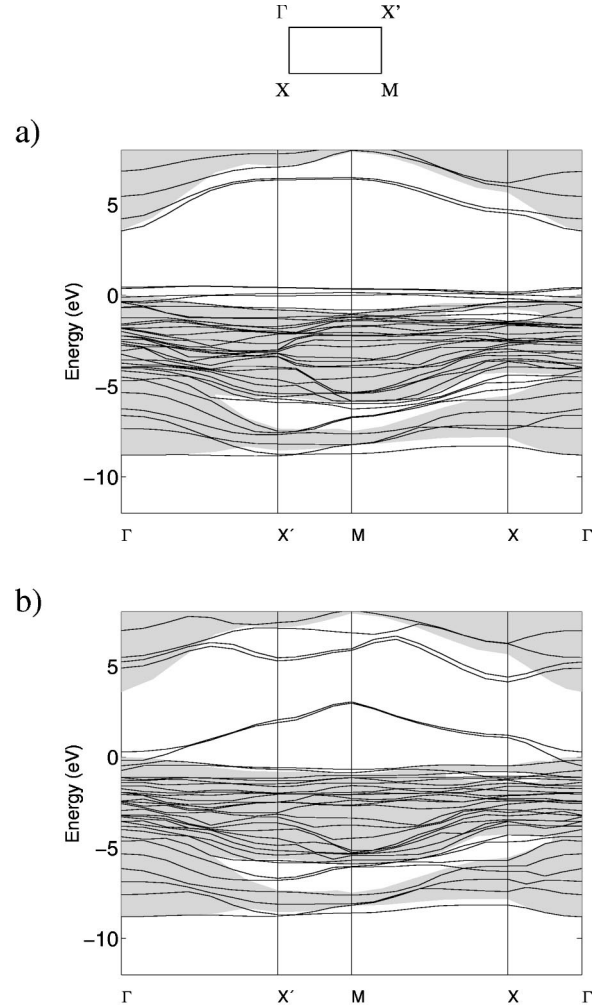


FIG. 3. Surface bands of the stoichiometric (a) and reduced (b) surface slab models calculated by using USP. The shaded region corresponds to the projected bulk band structure. The first Brillouin zone with high symmetry points is shown.

which are observed in Fig. 3(a). In the case of the reduced surface, occupied band gap states arise more significantly above the bulk valence band maximum as can be seen in Fig. 3(b). This is in agreement with photoemission measurements.^{31,41}

In order to study the electronic structure of reduced surfaces in more detail, we calculated their surface band structure and electron densities with both USP and PSP. By using USP, also density of states, Mulliken population analysis and bond populations were calculated. As shown in Fig. 3(b), band gap states are risen considerably (3 eV) above the valence band maximum at Γ point, and this rise was equivalently observed also in the case of PSP surface slab calculation. The reason for the dispersion is weak localization.¹⁰ The density maximum is found at about 2 eV above the valence band maximum at Γ point. In close agreement, photoemission investigations have suggested that filled gap states exist at 1.4 eV above the top of the valence band.³¹ According to the Mulliken population analysis the band gap states of the reduced surface are a mixture of mostly fourfold tin s and p types, containing also a slight O- p contribution.

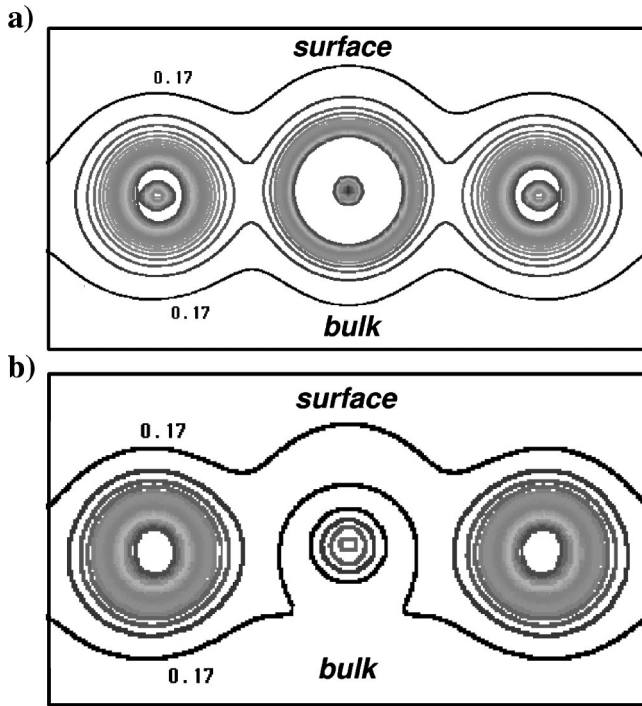


FIG. 4. Electron charge density viewed along [001] of the reduced surfaces calculated by using PSP (a) and USP (b). In-plane oxygen ions (left and right) and Sn^{2+} ion (at the middle) are shown, towards which charge increase stepwise, with steps of value $0.34 e/\text{\AA}^3$, starting from the outermost contours of charge $0.17 e/\text{\AA}^3$. The distances between Sn^{2+} ion and oxygen ions are 2.08 \AA in (a) and 2.11 \AA in (b), respectively.

The bond population analysis indicated for in-plane oxygen atoms that they are relatively strongly bound to the fivefold coordinated surface tin atoms and that their interaction to Sn^{2+} ions is reduced to be mainly of ionic nature.

The electron density of the reduced surfaces, at the (001) plane where it is most extended to the vacuum, is shown in Fig. 4(a). The quite uniform charge density at this plane, that was calculated by using PSP, was very similar in the case of the stoichiometric surface. When the charge distribution is compared to the calculation made for the reduced surface by using USP, differing valence electron densities in the vicinity of Sn^{2+} ions is observed as shown in Fig. 4(b). The difference may be viewed to be due to the better modelling of the Sn^{4+} ion core of the PSP.

V. CALCULATED OPTICAL PROPERTIES

From the calculated matrix elements of dipole optical transitions, the complex dielectric function ($\epsilon = \epsilon_1 + i\epsilon_2$) was evaluated as a function of transition energy up to 35 eV. The dielectric functions and absorption coefficient are represented in Figs. 5 and 6. The absorption spectrum of the bulk systems shown in Fig. 6 has two significant absorption maxima, which may be explained roughly in terms of the state densities discussed above and the selection rule ($\Delta l = \pm 1$) for direct transitions. Transitions at and below energy values of 10 eV originate from transitions from the upper valence band (Sn $5p$ -O $2p$ type) to Sn s conduction band.

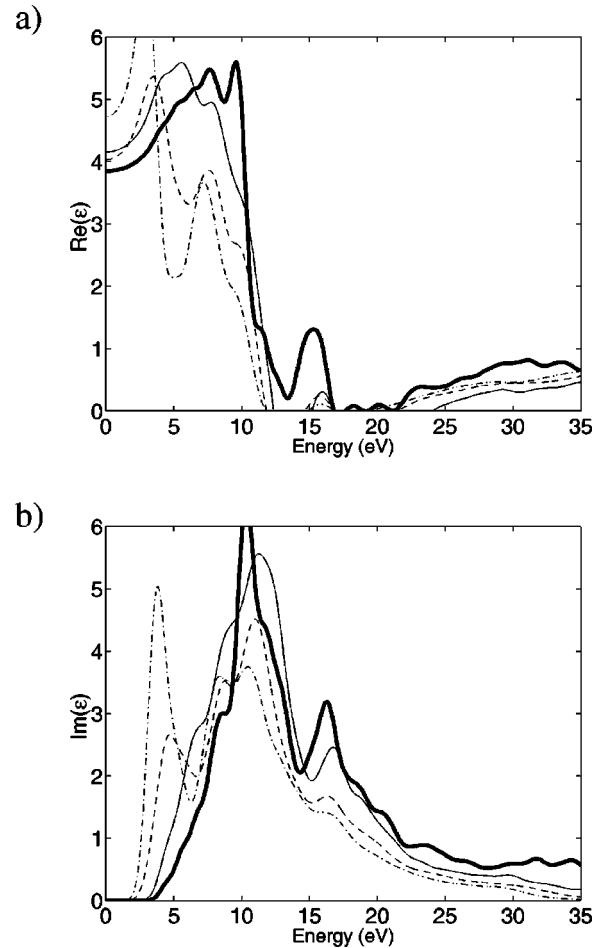


FIG. 5. Dielectric function ϵ_1 of bulk and surface systems as a function of excitation energy. The solid lines correspond to the bulk, obtained from calculations with PSP (thick line) and USP (thin line). The dashed line illustrates the case of stoichiometric slab and the dash-dot line the reduced slab, respectively.

The peak at 16 eV originates from lower valence band (Sn $5s$ -O $2p$) to Sn p conduction band. At higher excitation energies transitions also from the O $2s$ states become possible, which explains absorption above 20 eV. The PSP calculation clearly takes better into account allowed transitions from these and Sn $4d$ levels, since as seen in Fig. 2(a), more occupied states at valence band below -10 eV are accompanied. Experimental investigations have suggested^{30,31} that at about 32 eV Sn $4d$ -Sn $5p$ transitions contribute absorption, which explains the absorption of PSP at these energies in Fig. 6.

A comparison of the bulk and surface models indicates that ϵ_2 and α preserve the same features but are flatter in the case of the surface models. Both surface systems cause a decrease of the absorption edge, due to the surface states, to transition energies below 4 eV. Especially, in the case of the reduced surface, a significant feature in the ϵ_2 spectrum at energy below 5 eV is found. In experiments, surfaces contribute much less to absorption and this provides one argument supporting the fact that the surface transitions are associated to slightly higher transition energies (6 eV) in experiments.³⁰

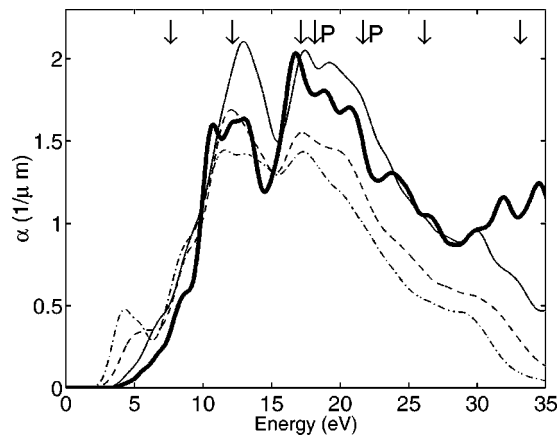


FIG. 6. Absorption coefficients α for bulk and surface systems as a function of excitation energy. The lines correspond to the ones used in Fig. 5. The arrows mark experimental absorption peaks (Ref. 30), with P indicating the plasmon related contributions.

A relevant result of absorption and ϵ_2 spectra is that other peaks observed in experimental measurements³⁰ could be found with even better precision. In experiments the transitions are associated to the energy values that are indicated by arrows in Fig. 6. As seen from the figure, except for energy values 17 and 25 eV, the agreement is better than 1 eV. Moreover, in experiments³⁰ the value of the absorption coefficient does not exceed $1.4 \mu\text{m}^{-1}$ and it is slightly overestimated in our calculations. Thus, the theory that we have implemented gives quite satisfactory results, although it excludes many of the microscopic effects. If instead of unpolarized light, polarization along [001] is assumed, absorption is in all our bulk and slab calculations smaller at transition energies below 7 eV. The absorption edge is shifted about 1 eV to higher energy values. In this respect, agreement with an other calculation made recently for bulk tin oxide⁴² is found.

VI. SUMMARY

Tin oxide bulk and two of its (110) surfaces were studied by utilizing density functional first principles calculations. The ultrasoft pseudopotential seems to predict geometry and electronic structure of bulk and surface systems in agreement with more accurate calculations performed. After correcting the band gap, also the agreement with experimental results is good. In the case of the stoichiometric surface, the bridging oxygens contribute occupied states near the top of the bulk valence band. In a case of reduced surface, filled states appear higher in the band gap, and are associated with weakly localized electron density of the fourfold coordinated tin Sn^{2+} ions. Both pseudopotentials, in agreement with some other density functional calculations, predict that these ions relax almost similarly outwards, but the coarse valence charge density in the vicinity of these ions differs slightly, however.

The ultraviolet optical properties calculation based on the calculation of dipole transition matrix elements, allows accurate predictions to be made for the absorption and the complex dielectric function. The surface contributes to the optical spectra by slightly washing out details and shifting the absorption edge to lower energy (below 4 eV) due to band gap states. A significant low-energy absorption peak appears close to the absorption edge and it is pronounced in a case of the reduced surface. The polarization direction of little absorption at lowest transition energies in tin oxide was found to correspond to [001] direction.

ACKNOWLEDGMENTS

We acknowledge the Academy of Finland for funding MECA project, within which this work has been carried out. We also acknowledge computational resources of the Center for Scientific Computing (CSC) Espoo, Finland.

- ¹Z.M. Jarzebski and J.P. Marton, *J. Electrochem. Soc.* **123**, 199C (1976).
- ²A.L. Dawar and J.C. Joshi, *J. Mater. Sci.* **19**, 1 (1984).
- ³C.L. Pang, S.A. Haycock, H. Raza, P.J. Möller, and G. Thornton, *Phys. Rev. B* **62**, R7775 (2000).
- ⁴V.E. Henrich and P.A. Cox, *The Surface Science of Metal Oxides*, (Cambridge University Press, Cambridge, 1994).
- ⁵S. Munnix and M. Schmeits, *Phys. Rev. B* **33**, 4136 (1986).
- ⁶T.T. Rantala, T.S. Rantala, and V. Lantto, *Mater. Sci. Semicond. Process.* **3**, 103 (2000); T.T. Rantala, T.S. Rantala and V. Lantto, *Surf. Sci.* **420**, 103 (1999).
- ⁷J. Goniakowski, J.M. Holender, L.N. Kantorovich, M.J. Gillan, and J.A. White, *Phys. Rev. B* **53**, 957 (1996).
- ⁸T.J. Godin and J.P. LaFemina, *Phys. Rev. B* **47**, 6518 (1993).
- ⁹T.S. Rantala, T.T. Rantala, and V. Lantto, *Sens. Actuators B* **65**, 375 (2000).
- ¹⁰I. Manassidis, J. Goniakowski, L.N. Kantorovich, and M.J. Gillan, *Surf. Sci.* **339**, 258 (1995).
- ¹¹J. Oviedo and M.J. Gillan, *Surf. Sci.* **467**, 35 (2000).
- ¹²D.F. Cox, T.B. Fryberger, and S. Semancik, *Phys. Rev. B* **38**, 2072 (1988).
- ¹³W.K. Choi, H. Sung, K.H. Kim, J.S. Cho, S.C. Choi, H.-J. Jung, S.K. Koh, C.M. Lee, and K. Jeong, *J. Mater. Sci. Lett.* **16**, 1551 (1997).
- ¹⁴M. Sinner-Hettenbach, M. Göthelid, J. Weissenrieder, H. von Schenck, T. Weiß, N. Barsan, and U. Weimar, *Surf. Sci.* **477**, 50 (2001).
- ¹⁵I. Lefebvre, M.A. Szymanski, J. Olivier-Fourcade, and J.C. Jumas, *Phys. Rev. B* **58**, 1896 (1998).
- ¹⁶Ph. Barbarat and S.F. Matar, *Comput. Mater. Sci.* **10**, 368 (1998).
- ¹⁷C. Noguera, *J. Phys.: Condens. Matter* **12**, R367 (2000).
- ¹⁸S. Gasirowicz, *Quantum Physics* (Wiley, New York, 1974).
- ¹⁹J.F. McGilp, *Prog. Surf. Sci.* **49**, 1 (1995).
- ²⁰(unpublished); V. Milman, B. Winkler, J.A. White, C.J. Pickard, M.C. Payne, E.V. Akhmatkaya and R.H. Nobes, *Int. J. Quantum Chem.* **77**, 895 (2000).

- ²¹D. Vanderbilt, Phys. Rev. B **41**, 7892 (1990).
- ²²K. Laasonen, A. Pasquarello, R. Car, C. Lee, and D. Vanderbilt, Phys. Rev. B **47**, 10 142 (1993).
- ²³M. Teter, Phys. Rev. B **48**, 5031 (1993).
- ²⁴J.P. Perdew and Y. Wang, Phys. Rev. B **46**, 6671 (1992).
- ²⁵G. Kresse and J. Furthmüller, Phys. Rev. B **54**, 11 169 (1996).
- ²⁶H.J. Monkhorst and J.D. Pack, Phys. Rev. B **13**, 5188 (1976).
- ²⁷W.H. Press, B. P. Flannery, S. A. Teukolsky, and W. T. Vetterling, *Numerical Recipes: The Art of Scientific Computing* (Cambridge University Press, Cambridge, 1989).
- ²⁸R.M. Hazen and L.W. Finger, J. Phys. Chem. Solids **42**, 143 (1981).
- ²⁹F. Wooten, *Optical Properties of Solids* (Academic Press, New York, 1981).
- ³⁰F. Yubero, V.M. Jiménez, and A.R. González-Elipé, Surf. Sci. **400**, 116 (1998).
- ³¹J.M. Themlin, R. Sporken, J. Darville, R. Caudano, and J.M. Gilles, Phys. Rev. B **42**, 11 914 (1990).
- ³²S.K. Song, Phys. Rev. B **60**, 11 137 (1999).
- ³³A.J. Read and R.J. Needs, Phys. Rev. B **44**, 13 071 (1991).
- ³⁴D. Sanchez-Portal, E. Artacho, and J.M. Soler, Solid State Commun. **95**, 685 (1995).
- ³⁵A. Svane and E. Antoncik, J. Phys. Chem. Solids **48**, 171 (1987).
- ³⁶A.E. Rakhshani, Y. Makdisi, and H.A. Ramazaniyan, J. Appl. Phys. **83**, 1049 (1998).
- ³⁷J. Robertson, J. Phys. C **12**, 4753 (1979); **12**, 4767 (1979).
- ³⁸J.-S. Lin, A. Qteish, M.P. Payne, and V. Heine, Phys. Rev. B **47**, 4174 (1993).
- ³⁹M. Ramamoorthy and D. Vanderbilt, Phys. Rev. B **49**, 16 721 (1994).
- ⁴⁰C.M. Freeman and C.R.A. Catlow, J. Solid State Chem. **85**, 65 (1990).
- ⁴¹D.F. Cox, T.B. Fryberger, and S. Semancik, Surf. Sci. **224**, 121 (1989).
- ⁴²Y. Mi, H. Odaka, and S. Iwata, Jpn. J. Appl. Phys. **38**, 3453 (1999).